

POLARIZED NEUTRONS AND STUDY OF MAGNETIC MATERIALS

S.V. Maleyev, A.I. Okorokov, G.P. Gordeyev, V.V. Runov

Since the beginning of the neutron physics the condensed matter studies were the main field of exploration of the Research Nuclear Reactors. So, after the decision of the construction of the WWR-M Reactor in Gatchina the organization of such studies became urgent. But at that time in the USSR the corresponding experience was very poor. Fortunately, however, there was an excellent theoretical background established by A.I. Akhiezer and I.Ya. Pomeranchuk in their seminal papers which were summarized in the book *"Certain problem of nuclear theory"* edited in Russia in 1950 [1]. Then in fifties S.V. Maleyev initiated by A.I. Akhiezer and I.M. Shmushkevich started his studies of the magnetic neutron scattering. Really it was the beginning of the neutron scattering theory in PNPI. On this theoretical background in the end of 1950s G.M. Drabkin, then a young scientist graduated as a nuclear physicist, began his prominent studies of the magnetic scattering of the polarized neutrons. It was time of fast growth of the Soviet Science and soon G.M. had an excellent crew of young collaborators including A.I. Okorokov, V.A. Trounov, G.P. Gordeyev, E.I. Zabidarov and then V.V. Runov, A.G. Gukasov, A.F. Schebetov, E.I. Maltsev, I.M. Lazebnick, L.A. Akselrod et al. At the same time S.V. Maleyev began to work with younger theoreticians V.A. Ruban, B.P. Toperverg, and A.V. Lazuta.

In the following we will discuss both experimental and theoretical results simultaneously. But in the beginning it is necessary to mention fundamental theoretical papers published in early 1960s by S.V. Maleyev in collaboration with Yu.A. Izyumov, V.G. Baryakhtar, and R.A. Suris [2–4] where the general analysis of the polarized neutron magnetic scattering was presented. Similar results were published by M. Blume [5]. Then two experimental approaches to the polarization neutron scattering were developed completely based on these theoretical studies.

In the first approach developed in the seminal paper [6] and known as the linear neutron polarimetry the polarized neutrons scatter in the sample which is in a guiding magnetic field and then the spin-flip and non-spin-flip intensities are measured. The deficiency of this method is that one cannot discriminate between change of the absolute value of the neutron polarization and its rotation. So the three-dimensional analysis of the neutron polarization was developed. In this case the initial neutron polarization is set subsequently in three mutually perpendicular directions and then after scattering on the sample in the zero magnetic field three components of the neutron polarization are measured. This more sophisticated technique was developed in the beginning of the 1970s by Th. Rekveldt for the transmitted beam [7] and by G.M. Drabkin, A.I. Okorokov et al. for the small-angle scattering [8,9] (see Fig.1). More later the device for the large-angle scattering and magnetic structure studies (CRYOPAD) was developed in ILL by F. Tasset et al. [10].

In 1965 the methodical stage was finished and real physical studies was began. Observation of the spin reversion at the small angle critical scattering in iron [11] was the first experimental confirmation of the famous Halpern–Johnson expression for the polarization of the scattering neutrons in the case of the magnetically isotropic sample [12]

$$\mathbf{P} = -\mathbf{e}(\mathbf{eP}_0) , \quad (1)$$

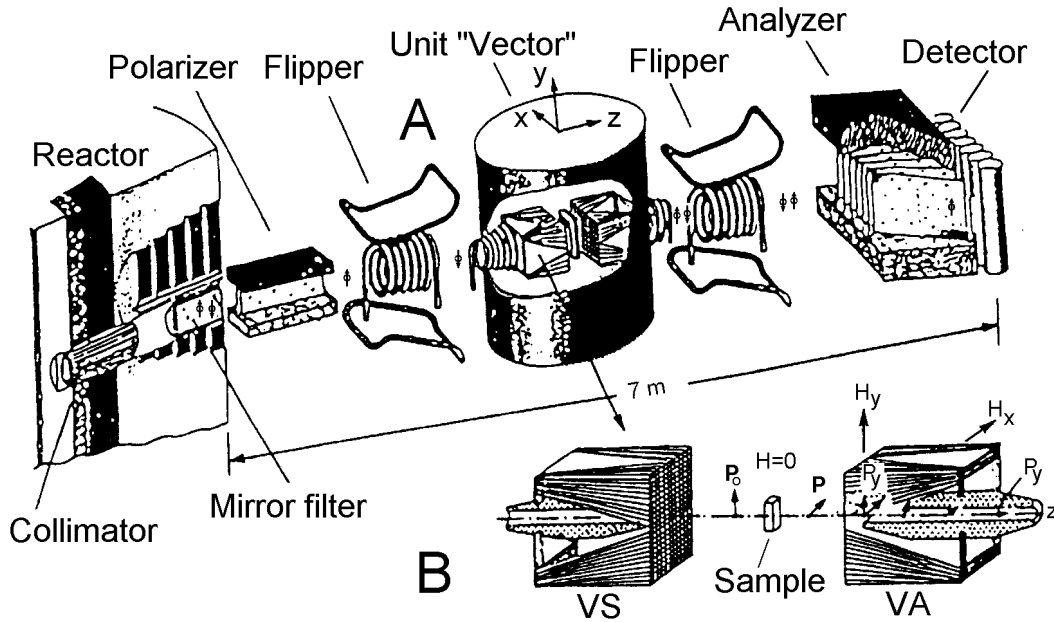


Figure 1: "A" is a block-scheme of the small-angle scattering set-up with the three-dimensional analysis of scattered neutron polarization. "B" is a unit "vector": specifying (VS) and analysing (VA) units and examples for measuring the P_y component of polarization are shown

where \mathbf{P}_0 and \mathbf{P} are initial and final neutron polarizations and $\mathbf{e} = \mathbf{q}/q$ is the unit vector along the momentum transfer \mathbf{q} (see Fig.2).

It was shown in [13] that such experiments allow to study components of neutron polarization

$$\begin{aligned}
 P_z &= -P_0 \int d\omega \frac{\omega^2}{\omega^2 + (2E\vartheta)^2} \frac{\sigma(\vartheta, \omega)}{\sigma(\vartheta)} \\
 P_x &= -P_0 \int d\omega \frac{(2E\vartheta)^2}{\omega^2 + (2E\vartheta)^2} \frac{\sigma(\vartheta, \omega)}{\sigma(\vartheta)}, \quad (2)
 \end{aligned}$$

where z and x are axes directed along and perpendicular to the incident beam in the scattering

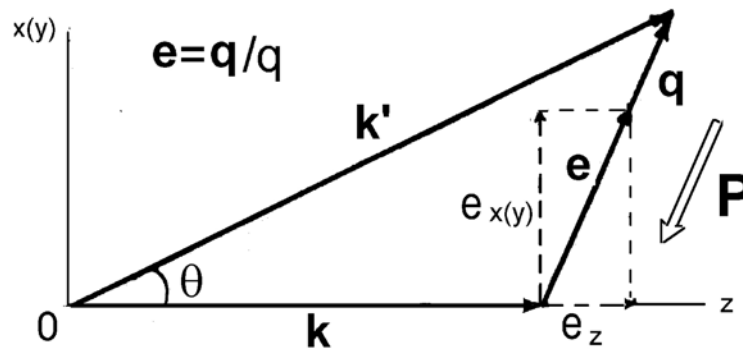


Figure 2: Scheme of small-angle polarized neutron scattering. \mathbf{P} is the direction of magnetic neutron scattered polarization

plane, $\sigma(\vartheta)$ is the total scattering cross sections at the angle $\vartheta \ll 1$, and E is the incident neutron energy [13].

Using three-dimensional analysis one can measure along with intensity $\sigma(\vartheta)$ two other quantities $P_x\sigma$ and $P_z\sigma$, connected by the sum rule

$$P_x + P_z = -1 . \quad (3)$$

In the expressions for P_x and P_z the contribute energies are $\omega \lesssim 2E\vartheta$ and $\omega \gtrsim 2E\vartheta$ respectively. Hence, P_x and P_z are connected to the quasielastic and strongly inelastic scattering events respectively.

In the case of the critical scattering in ferromagnets a conventional determination of the correlation length demands very careful estimation of the inelasticity [14]. The natural energy cutoff in the expression of P_x allows to avoid this complication and to determine this length in iron in much larger temperature range as before. At the same time, by measuring P_z one can investigate the large ω region, which cannot be studied by the conventional inelastic scattering experiments.

In subsequent years the following research areas were developed:

1. Vector analysis of polarization of scattered neutrons.
2. Neutron depolarization as a tool for the investigation of the large-scale magnetic inhomogeneities which cannot be resolved in conventional scattering experiments, and Larmor precession experiments.
3. Small-angle scattering of polarized neutrons in disordered magnetic systems.
4. Investigation of the dynamical chiral spin fluctuations. It should be stressed here that this method was an achievement of PNPI researchers and provided in principle new physical information which cannot be obtained in the other neutron scattering experiments.
5. The problem of colossal magnetoresistance.

1. Vector analysis of scattered neutrons

It follows from Eq.(2), that the degree of the inelasticity given by ratio

$$R = \frac{P_z}{P_x} \approx \frac{\langle \omega^2 \rangle}{(2E\theta)^2} , \quad (4)$$

provides information on the wide inelastic region of ω , which cannot be measured in the conventional inelastic scattering experiments [14].

For the self-consistent data analysis we used the sum rule (3) and following equations:

$$I = I_m + I_n + I_b , \quad P_i I = P_{mi} I_m + P_{ni} I_n + P_{bi} I_b , \quad (5)$$

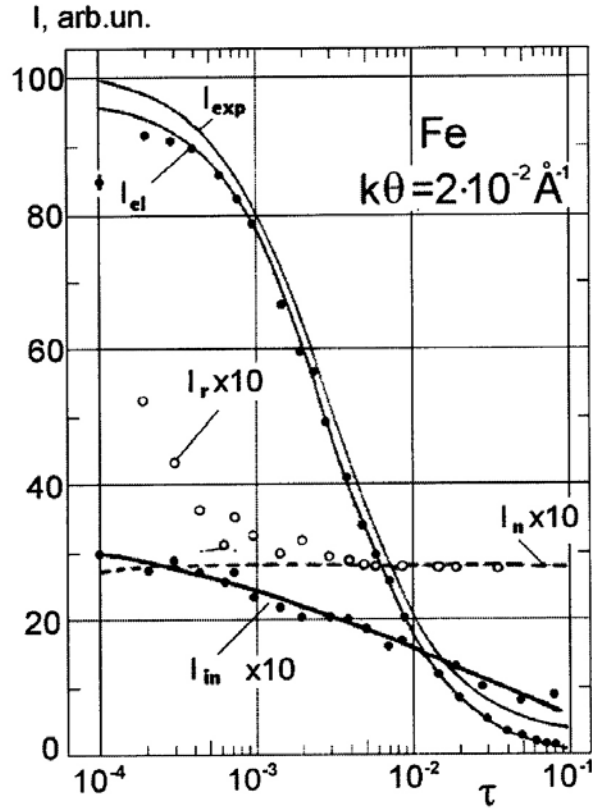


Figure 3: Temperature dependence of different parts of the intensity: I_{exp} is experimental total scattering (solid line); I_{el} is "elastic" magnetic scattering (points); I_{in} is "inelastic" magnetic scattering; I_n is nuclear scattering, extrapolated to T_c from $T > T_\gamma$, where $T_\gamma = 1183\text{K}$ is the temperature of transition in nonmagnetic γ -phase (dashed line); $I_r = I_{exp} - I_{el} - I_{in}$ is residual scattering (open points). The solid line of I_{el} is Ornstein-Zernike fit for $\tau > 5 \cdot 10^{-4}$ (see text). The additional scattering intensity $I_r - I_n$ is interpreted as multiple magnetic scattering [15]

where I_m and I_n are intensities of magnetic and nuclear scattering, and I_b is an experimental background. With help of this and according to Eqs. (2) for "elastic" (I_{el}) and "inelastic" (I_{in}) parts of magnetic scattering we have

$$I_{el} = -P_{mx} I_m , \quad (6)$$

$$I_{in} = -P_{mz} I_m . \quad (7)$$

Experimental intensity I_{exp} as function of $\tau = (T - T_c)/T_c$ at $k\theta = 2 \cdot 10^{-2} \text{\AA}^{-1}$ is shown in Fig.3 along with I_{el} and I_{in} for Fe. The residual intensity $I_r = I_{exp} - I_{el} - I_{in}$ should coincide with the nuclear intensity I_n (dashed line in Fig.3), which is defined in nonmagnetic γ -phase at $T > T_\gamma = 1183\text{K}$ and extrapolated to T_c . For $\tau > 3 \cdot 10^{-3}$ this is the case, but near T_c this equality is violated. As it was shown in Ref. [15], this additional intensity $I_r - I_n$ is a result of multiple magnetic scattering which appears near T_c .

It is well known that the problem of multiple scattering is very difficult to resolve by conventional methods. In the case of polarized neutrons a contribution of the double critical magnetic scattering in ferromagnets to the neutron polarization P was calculated by Toperverg,

(Ref. [15]), and correction term Δ to the sum rule was determined

$$\Sigma P_i = -1 + \Delta , \quad (8)$$

where Δ depends on experimental parameters only: the intensity of the critical scattering at $q = 0$, correlation length κ and the sample thickness L .

Following Ref. [14] in the critical region above T_c we represent the cross section as follows

$$\sigma(q, \omega) = A(q^2 + \kappa^2)^{-1} F(q, \omega) , \quad (9)$$

where κ is the inverse correlation length, A is a constant, and F is a dynamical form-factor normalized by the condition $\int d\omega F(q, \omega) = 1$. In the case of the second order phase transition $\kappa = a^{-1}\tau^\nu$, where a is of order of interatomic spacing, $\tau = (T - T_c)/T_c$, and ν is the correlation length critical exponent. In the small-angle neutron scattering (SANS) experiment the ω integrated cross section has the Ornstein-Zernike form given by the first factor in Eq.(9), if one can neglect dependence of ω on q . However, as $\tau \rightarrow 0$ for determination of κ one should perform measurements at very small $k\vartheta$, where the ω dependence on q becomes important. Meanwhile, as we demonstrated above there is a natural cut off of the large ω in the elastic part of the scattering (see Eq.(2)). Hence, it is more appropriate for determination of κ . Corresponding results are shown in Fig.4(1) along with the results of the conventional scattering experiments [14,16,17]. We confirmed the prediction of the scaling theory up to $\tau \simeq 10^{-4}$, while conventional method failed to do it for $\tau < 2 \cdot 10^{-3}$.

The τ dependence of the average transferred energy $\langle \omega^2 \rangle^{1/2} = 2E\vartheta R^{1/2}$ for $\vartheta = 34'$ is shown in Fig.4(2). We calculate this dependence using the Lorentzian $F(q, \omega) = \Gamma_q / [\pi(\omega^2 + \Gamma_q^2)]$ with the Resibois-Piette form for Γ_q : $\Gamma_q = Cq^z [\exp(\kappa R_1/q) + R_2(\kappa/q)]^{1/2}$ with $C = 130 \text{ meV} \text{ \AA}^{5/2}$, $R_1 = -1.83$ and $R_2 = 0.43$ (dashed line in Fig.4(2)) [18,19]. The inelastic scattering data are described by this form for $\omega \sim \Gamma_q$ [20]. In our case of the large transferred energies much better fit of the data attains, if $C = 106 \pm 5 \text{ meV} \text{ \AA}^{5/2}$, $R_1 = -3.7 \pm 0.3$ and $R_2 = 1.01 \pm 0.05$. Hence, we demonstrate that the Lorentzian is not appropriate for description of the tail of the form-factor $F(q, \omega)$ at $\omega \gg \Gamma_q$. The same conclusion was done using polarized neutron scattering in iron [21]. Theoretical arguments show that at $\omega \gg \Gamma$ the form-factor $F(q, \omega) \sim q^2/\omega^{8/5}$ [22]. However we cannot check this prediction because of restricted range of available $k\vartheta$.

2. Neutron depolarization and Larmor precession

In the classical paper by Halpern and Holstein [23] the neutron depolarization was considered as a result of small rotations of the neutron spin in the field of magnetic inhomogeneities of the sample. However, if neutron passes through inhomogeneity its coordinate is determined with accuracy of order d , where d is the size of the inhomogeneity and the neutron momentum acquires uncertainty \hbar/d . Hence, interaction with the inhomogeneity may be considered as a small-angle scattering rather than classical rotation. Using this simple idea the quantum theory of the depolarization was developed [24–26]. Observation of the anisotropy of depolarization was the most important result of this approach. Namely it was shown that in magnetically isotropic sample the neutrons are depolarized stronger, if they were polarized perpendicular

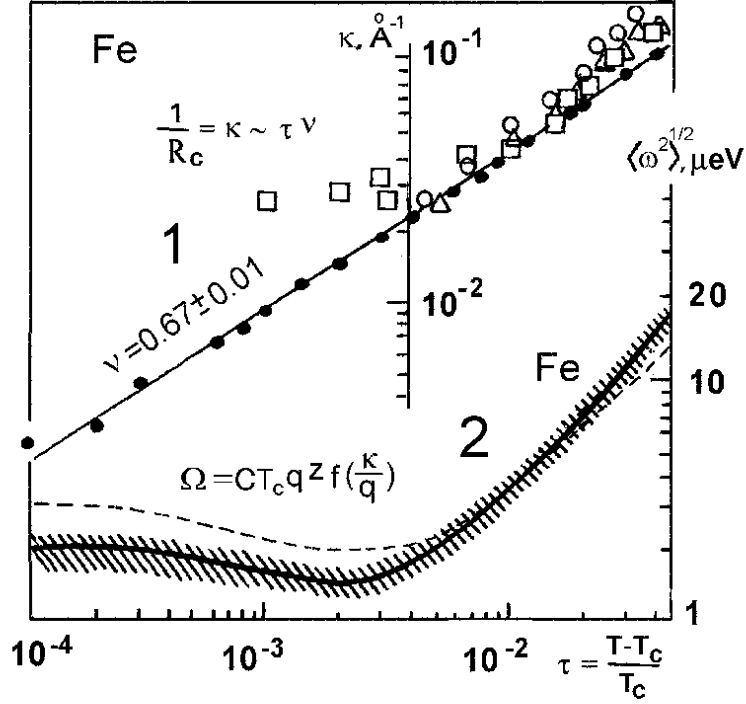


Figure 4: Some results obtained by VA-SAPNS in iron above T_c : 1. Inverse correlation radius $\kappa = 1/R_c$ (black points). The results of conventional SANS experiments are shown for comparison: (\circ) is [14], (\square) is [16], (Δ) is [17]. 2. Inelasticity $R = P_z/(P_x + P_y)$ in units of $\langle\omega^2\rangle^{1/2}$ at $k\theta = 2 \cdot 10^{-2} \text{ \AA}^{-1}$. The shaded area is the confidence interval for experimental data. Solid line is the best fit curve with free parameters of Resibois and Piette (RP) scaling function Ω (see text). The dashed line is a calculation using parameters of RP scaling function [19]

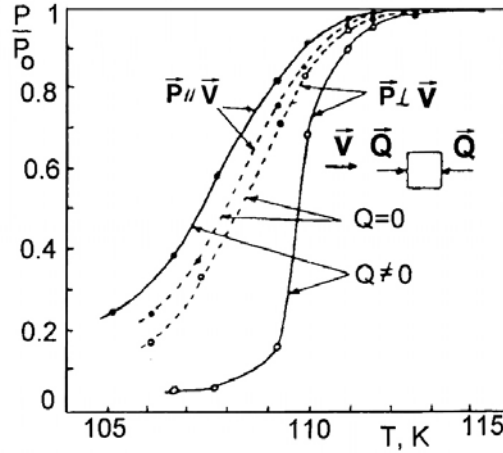


Figure 5: The dependence of $P(T)$ in alloy Pd-Fe (4 at.%) near T_c without loading ($Q = 0$) and at uniaxial compression ($Q \neq 0$)

to the beam. This result is a direct consequence of Eq.(1). Indeed, for the elastic small-angle scattering \mathbf{e} is perpendicular to the beam. Hence, if \mathbf{P}_0 is directed along the beam, the scattered neutrons are depolarized, but if \mathbf{P}_0 is perpendicular to the beam, the polarization changes sign and diminishing of the polarization becomes stronger. The theory predicts that $\ln(P_{\perp}/P_{0\perp})/\ln(P_{\parallel}/P_{0\parallel}) = 3/2$. This simple relation was confirmed experimentally in the case of the depolarization in the nickel powder [9].

In the case of magnetically anisotropic sample there is rather complex dependence of the depolarization on the mutual orientation of the initial polarization, beam direction and the anisotropy axis [25,26]. This phenomenon investigated in the ferromagnetic compound PdFe near T_c (4 at.% of Fe), where the magnetic anisotropy appears as a result of the external pressure. It was shown that this pressure provoked the easy-plane anisotropy [27] (see Fig.5). Hence, the investigation of the anisotropy of the depolarization gives a possibility to study the magnetic texture of the sample and its dependence on the external conditions.

In conventional ordered ferromagnets such as Fe or Ni the depolarization above T_c is negligibly small, as the average magnetization of the critical fluctuations is low [24–26]. This result was confirmed experimentally in the critical scattering in Ni and Fe [28]. However recently it was shown that this is not the case for the invar alloys $\text{Fe}_{70}\text{Ni}_{30}$ and $\text{Fe}_{65}\text{Ni}_{35}$, where the depolarization is strong well above T_c [29]. This phenomenon was explained by the existence of two magnetic correlation lengths (Fig.6).

It was the first observation of the two-length behaviour in the magnetic phase transition, which is well known in the nonmagnetic disordered systems (see for example [30]). Further investigation of this phenomenon using small-angle scattering and depolarization in the magnetized sample allows to explain this two-length scale phenomenon by the fluctuations of the Curie temperature in the sample due to the spatial disorder and to estimate the value $(\Delta T_c)^2/T_c^2$ [31] (Fig.7).

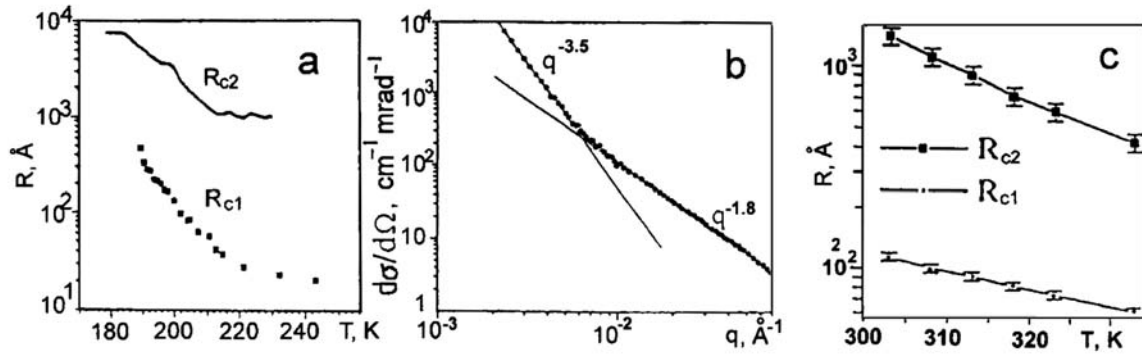


Figure 6: "a" is temperature dependence of R defined by neutron scattering at $q > 10^{-2} \text{\AA}^{-1}$ (R_{C1}) and by neutron depolarization (R_{C2}) in invar alloy $\text{Fe}_{75}\text{Ni}_{25}$ ($T_c = 190 \text{ K}$). "b" is q -dependence of neutron scattering cross section in $\text{Fe}_{70}\text{Ni}_{30}$ ($T_c = 285 \text{ K}$) at room temperature. One can see two different scales. "c" is T -dependence of correlation radii R_{C1} and R_{C2} in $\text{Fe}_{70}\text{Ni}_{30}$ defined from neutron scattering (b)

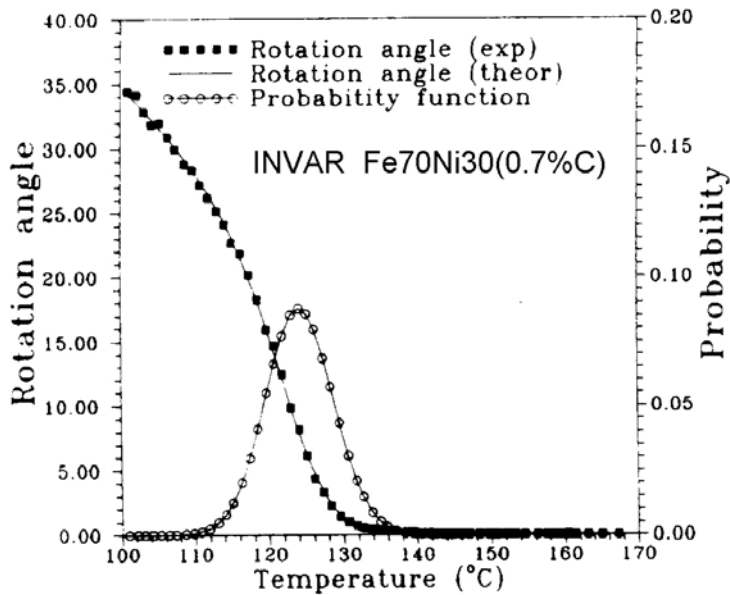


Figure 7: The temperature dependences of rotation angle of polarization vector \mathbf{P} and probability function of local T_c in invar alloy $\text{Fe}_{70}\text{Ni}_{30}$ (0.7 at.% C)

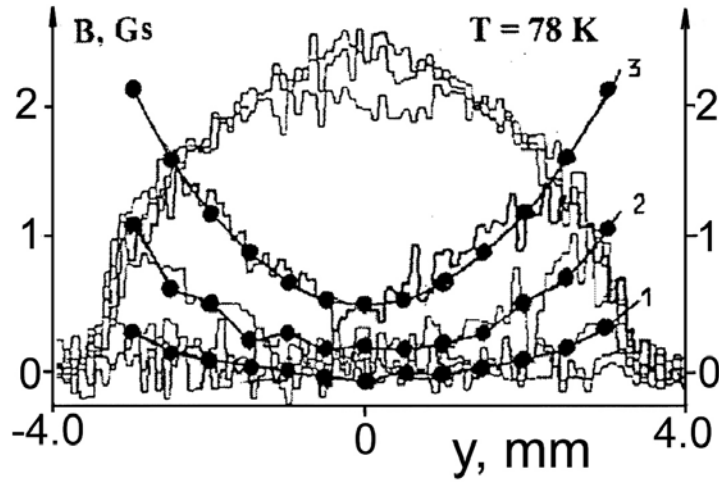


Figure 8: Visualization of magnetic flux B in Y-Ba-Cu-O ceramics with external magnetic field switched on (curves 1,2,3 for $H = 2.2, 3, 1$ and 4 Oe, respectively) and switched off (trapped flux) for values of H from 0.45 to 7.2 Oe

By means of Larmor precession of polarization vector \mathbf{P} in a homogeneities magnetic field \mathbf{B}

$$\frac{d\mathbf{P}(t)}{dt} = \gamma [\mathbf{P}(t), \mathbf{B}]$$

one can define the value $\langle B \rangle$ by measuring rotating angle $\varphi = \gamma \frac{BL}{v}$, where γ is gyromagnetic relation, L is the length of the sample along the beam and v is the neutron velocity. The idea was used for investigation of the internal field B distribution in a ceramic sample of Y-Ba-Cu-O which is a good example of the Josephson medium [32]. The sample was scanned by narrow beam of polarized neutrons. Shown in Fig.8 the distributions of the magnetic field penetration in the sample as well as the trapped magnetic flux when the external field is switched off. The range of applied fields was $H_{C1} < H < H_{C2}$. The patterns of the B distribution are in agreement with Bean law: i) small field penetrate to the sample on a limited depth and distribution of trapped field has two maxima near edges of the sample; ii) the larger field penetrates up to center of the sample and there is only one maximum.

From Maxwell equations we can calculate the corresponding current density $J_{\perp}(B)$

$$J_{\perp}(B) = \frac{1}{4\pi} \frac{\partial B}{\partial y}. \quad (10)$$

Internal field dependencies of the current density are shown in Fig. 9. Maximal value of J_{\perp} is the critical current density J_{C1} .

The experiments with vector analysis allowed to visualize not only the transverse current J_{\perp} but also the longitudinal one J_{\parallel} :

$$J_{\parallel} = \frac{B}{4\pi} \frac{\partial \alpha}{\partial y}, \quad (11)$$

where α is the rotation angle of trapped field \mathbf{B} .

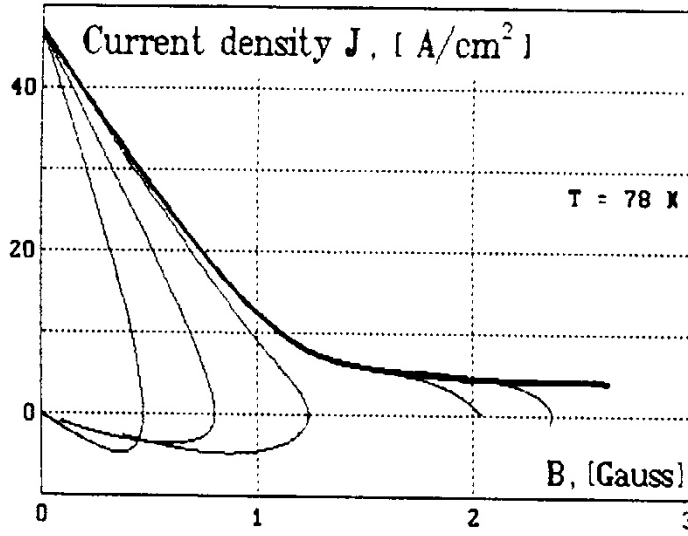


Figure 9: Internal field dependences of the current density at $T = 60$ K. Thick line corresponds to the distribution of $B(y)$ at $H \geq H_{C2}$

The problem of longitudinal currents in conventional type-II superconductors has been considered by several authors [33,34]. It was demonstrated that considering only the vortices pinning leads to the conclusion that longitudinal (with respect to the magnetic field direction) critical current $J_{C\parallel}$ is infinite (namely, $J_{C\parallel} = J_{\text{pair}}$, where J_{pair} is the dispairing current), but the longitudinal electric field E_{\parallel} is always equal to zero. This case corresponds to the so-called force-free configurations. But the experiment demonstrates that $J_{C\parallel} \sim J_{C\perp}$, where $J_{C\perp}$ is the transverse critical current, and $E_{\parallel} \neq 0$ at penetrating of a magnetic field in the superconductor. If one assumed that the vortex matter can only be deformed, then it would not be possible to explain these facts. In order to explain them, the flux-line cutting (FLC) model has been proposed [34]. Its essence is that the vortices appearing at the surface which are not parallel to the vortices in the bulk, they penetrate into the sample by intersecting, and subsequently, cross-joining with adjacent vortices. As a result of FLC, finite $J_{C\parallel}$ and $J_{C\perp}$ as well as E_{\parallel} and E_{\perp} occur.

Experimentally the possibility to measure J_{\parallel} was realized by rotation of external field H on angle ϕ before its switching off. One of the experimental result at $T = 60$ K, $H = 7.5$ Oe and $\phi = 45^\circ$ is shown in Fig. 10 [35]. Here $\alpha = 0$ is direction of \mathbf{B} in the beginning of rotation of external field H (at the $\phi = 0$).

From the distributions of B and α the currents J_{\perp} and J_{\parallel} were calculated from the first principles (eqs. (10) and (11)). It is seen that they are of the same order of magnitude (Fig.10c).

The main result of this work is the demonstration of some qualitative phenomena which take place in a Josephson medium under rotation of a sufficiently weak external field. The gradient of the inclination angle of B which is clearly seen in the experiment can be explained only by the presence of a persistent longitudinal current. In precisely the same way, the observation of a gradient of the value of $B(x)$ shows the presence of a persistent transverse current. The most important result is the demonstration of the longitudinal current which is predicted by

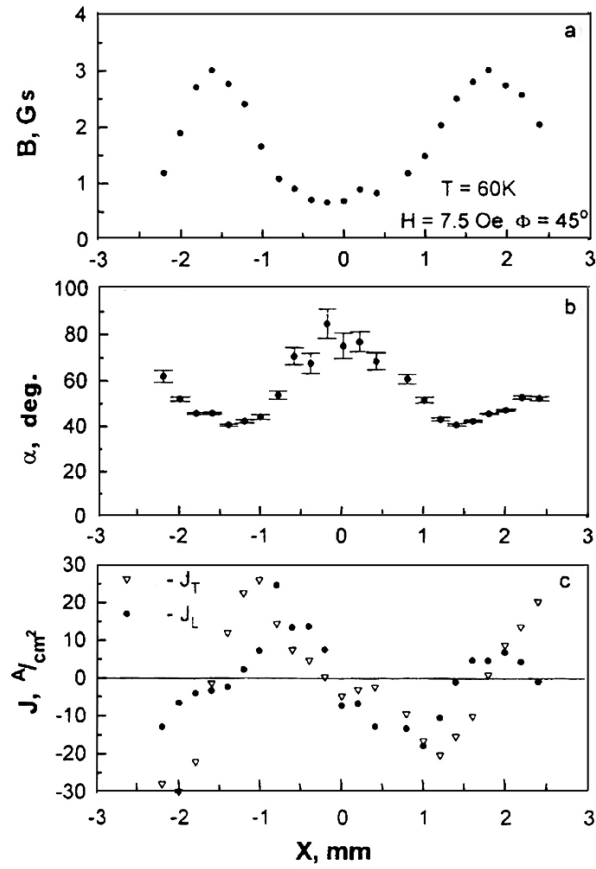


Figure 10: Sample scan for the external field rotation angle $\phi = 45^\circ$: (a) induction B ; (b) angle α ; (c) currents $J_T \equiv J \perp$ and $J_L \equiv J_{\parallel}$

the aforementioned simplified model.

3. Small-angle scattering of polarized neutrons in disordered magnetic systems

As the example of investigation of disordered magnetic system we should remark the work [36]. In that work the theory of spin correlations in concentrated spin-glasses systems was developed and the experimental measurements in concentrated $\text{Fe}_{80-x}\text{Ni}_x\text{Cr}_{20}$ spin-glasses alloys were made by the method of small-angle polarized neutron scattering.

In 80s there was a considerable interest in spin glass systems (SG) such as dilute ("classical") spin glasses of the $\text{Mn}_x\text{Cu}_{1-x}$ type, and also in concentrated spin systems with competing random interaction, such as $\text{Eu}_x\text{Sr}_{1-x}\text{S}$, $(\text{Fe}_x\text{Mn}_{1-x})\text{P}_{16}\text{B}_6\text{Al}_3$, $\text{Fe}_x\text{Cr}_{1-x}$, etc. Later, depending on the concentration x , the sequence of the phase transitions is displayed: paramagnetic (PM), ferromagnetic (FM) and reentrant spin glass phase (PSG). In magnets with random competing interactions the frozen spin fluctuations along with the ordinary thermodynamic fluctuations occur at transition to the FM, SG or RSG phases. It is very important to note that in SG (RSG) phases the frozen fluctuations relax slowly. It is the most important property of the spin-glass state which is in principle nonequilibrium, nonergodic and is characterized by the following experimentally observed irreversible effects: magnetic viscosity, magnetic memory, etc. According to the current ideas, these slow spin relaxation effects are due to the existence of the macroscopically large number of degenerate low-energy states (valleys). The distributions of valleys give rise to a broad spectrum of relaxation times and a logarithmically slow evolution of both homogeneous quantities (magnetization, susceptibility, etc.) and also of inhomogeneous spin correlations.

In our performed experiments the $\text{Fe}_{80-x}\text{Ni}_x\text{Cr}_{20}$ systems exhibit the sequence of PM-FM-RSG phase transitions. It was found that not only usual thermodynamic but also frozen spin configuration correlations must be taken into account for description of small-angle scattering in low temperature (RSG) phase of such magnetic materials. The typical data are shown in Fig.11, where the solid line on scattering data (1) is the best-fit by the equation followed from theory [36]:

$$I(q) = \int dp K(p, \kappa) R(q - p) . \quad (12)$$

Here, $R(q - p)$ is the resolution function of the small-angle device, and $K(p, \kappa)$ is the sum of two terms:

$$K(p, \kappa) = \frac{A_1}{(p^2 + \kappa^2)^2} + \frac{A_2}{(p^2 + \kappa^2)} . \quad (13)$$

The first term in this expression describes the contribution of the configuration correlations, whereas the second one corresponds to the thermodynamic correlations. Furthermore, it was found that not only correlation radius $R_c = \kappa^{-1}$ depends on the relative temperature in accordance with the scaling assumption, but the parameter A_1 also is changed as a power of τ .

The spin relaxation effects on $\text{Fe}_{80-x}\text{Ni}_x\text{Cr}_{20}$ systems were studied too. The slow logarithmic relaxation of the polarization between two states with different magnetic treatments, ZFC and FC (2 and 3 in Fig.12) was found.

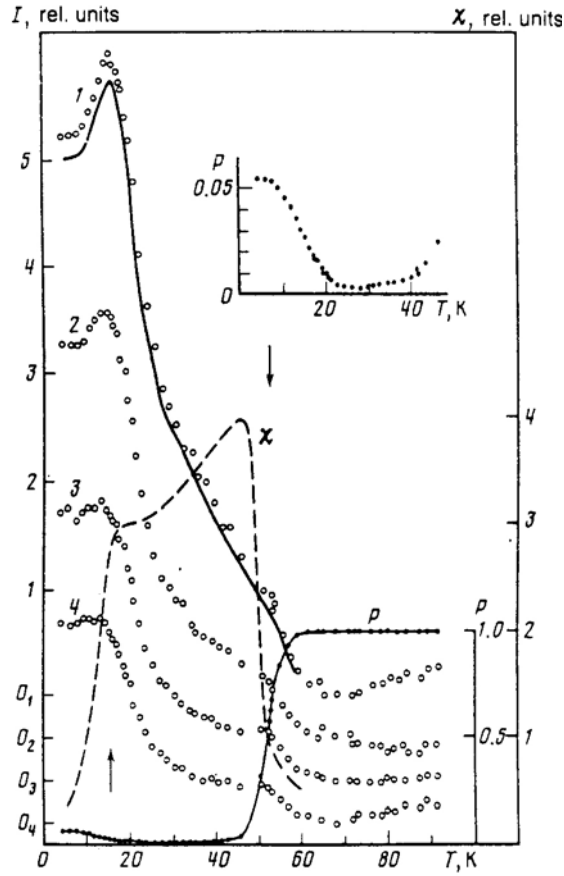


Figure 11: Temperature dependences of the intensity of the neutron scattering I , of the neutron polarization P , and of the magnetic susceptibility χ of the alloy with $x = 26$; 1) $q = 4.8 \cdot 10^{-3} \text{ \AA}^{-1}$; 2) $5.8 \cdot 10^{-3} \text{ \AA}^{-1}$; 3) $7.4 \cdot 10^{-3} \text{ \AA}^{-1}$; 4) $8.5 \cdot 10^{-3} \text{ \AA}^{-1}$. The upward arrow identifies the position of the scattering maximum T_m characterized by the minimum transferred momentum, and the downward arrow identifies T_c . The continuous curve is the dependence $I(T)$ calculated for $q = 4.8 \cdot 10^{-3} \text{ \AA}^{-1}$. The indices of zeros (on the left) denote the positions of zeros of curves labelled by the relevant numbers

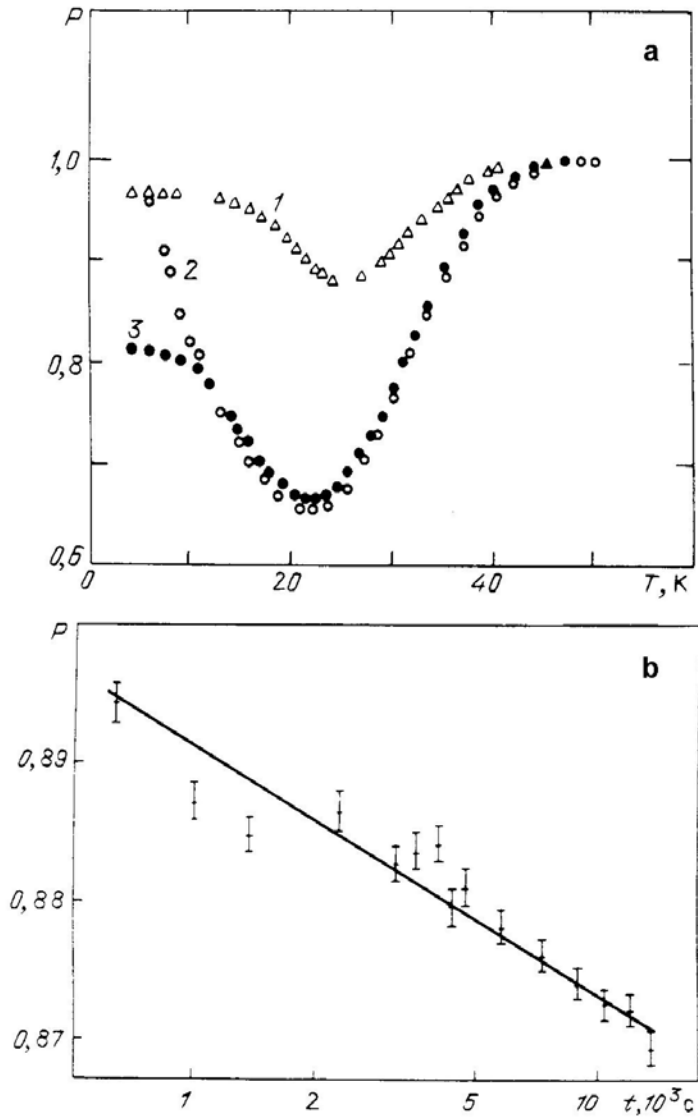


Figure 12: "a" is polarization $P(T)$ of neutrons transmitted through the sample $\text{Fe}_{56}\text{Ni}_{24}\text{Cr}_{20}$: 1 is in "zero" magnetic field; 2 is in the field $H_x = 62$ Oe after preliminary cooling to 4.2 K in zero field; 3 is measuring in the field $H_x = 62$ Oe. "b" is the long-time logarithmic relaxation from state 2 to state 3 (curves in "a") at $T = 8$ K: $P(t) = P_2 - S \ln(t/t_0)$, where S is a coefficient of consequence

4. Chiral spin fluctuations and polarized neutrons

It is well known that the conventional magnetic scattering is determined by the symmetric part of generalized magnetic susceptibility, which describes the two-spin correlations. In this case the cross section is independent on the initial neutron polarization \mathbf{P}_0 . Hence, the magnetic neutron scattering provides information on the two-spin fluctuations only. However in any strongly correlated spin system there are higher order spin fluctuations but they cannot be studied in the conventional neutron scattering experiments. The situation is changed in the presence of external magnetic field or spontaneous magnetization of the sample. In this case the projection of the chiral spin fluctuations described by the vector product $\mathbf{S}_{\mathbf{k}} \times \mathbf{S}_{-\mathbf{k}}$, on the sample magnetization \mathbf{S}_0 where $\mathbf{S}_{\mathbf{k}}$ is the Fourier transform of the spin density, gives rise to the antisymmetric part of the spin susceptibility, which contributes to the \mathbf{P}_0 dependent part of the cross section [37,38]. It is related to the spin chirality $\mathbf{S}_{\mathbf{k}} \times \mathbf{S}_{-\mathbf{k}}$ and disappears at $\omega = 0$. So it was named as Dynamical Chirality (DC). As the DC is related to the three-spin correlations, it has to provide new physical information, which cannot be obtained in conventional neutron scattering experiments. Later we present some examples of the investigation of the DC in ferromagnets. Recently similar studies were undertaken for the triangular lattice antiferromagnets and helimagnetic holmium and for the first time chiral critical exponents were determined experimentally [39,40]. The description of these studies one can find in this issue [41].

The chiral contribution to the cross section has the form

$$\sigma_{ch}(\mathbf{Q}, \omega) = \frac{2}{\pi} [r f(\mathbf{Q})]^2 \left(\frac{k_f}{k_i} \right) (1 - e^{-\omega/T})^{-1} (\mathbf{P}_0 \mathbf{Q}) (\mathbf{Q} \hat{h}) \text{Im } S(\mathbf{Q}, \omega). \quad (14)$$

where \hat{h} is the unit vector along the field, $\text{Im } S$ is an even function of ω due to t -oddness of \mathbf{H} . As a result $\sigma_{ch}(\omega)$ changes sign with ω [37,38]. This was confirmed experimentally for critical scattering in iron [42,43] and triangular-lattice antiferromagnets CsMnBr_3 and CsNiCl_3 [44]. If for given \mathbf{Q} the characteristic energy $\omega \ll T$, the static chiral scattering is zero:

$$\sigma_{cg}(\mathbf{Q}) = \left(\frac{T}{\pi} \right) \int_{-\infty}^{\infty} \left(\frac{d\omega}{\omega} \right) \sigma_{ch}(\mathbf{Q}, \omega) = 0. \quad (15)$$

However one can avoid this disappointing result changing weights of positive and negative ω contributions to the integral. For the small-angle scattering it may be done if the magnetic field is inclined to the direction of the incident beam. Indeed, if the field lies in the scattering plane at angle ψ to the beam direction and \mathbf{P}_0 is along the field, the kinematic factor in Eq.(15) before $\text{Im } S$ contains the term equal to $(2E\vartheta\omega P_0 \sin 2\psi)/[\omega^2 + (2E\vartheta)^2]$ where ϑ is the scattering angle, E is the neutron energy and $\omega \ll E$. As a result instead of (16) one gets

$$\sigma_{ch}(\vartheta) = [r f(\mathbf{Q})]^2 \frac{4ET P_0 \sin 2\varphi}{\pi} \int d\omega \frac{\text{Im } S_H(k_i \vartheta, \omega, H)}{\omega^2 + (2E\vartheta)^2}. \quad (16)$$

Obviously this contribution may be easily extracted experimentally due to its dependence on P_0 and ϑ . This method was created in PNPI [45–47] and was called as a method of "left-right asymmetry" (LRA) of polarized neutron scattering. Using this method several new results were obtained which cannot be achieved using conventional neutron scattering. We present below some of them.

4.1. Polyakov-Kadanoff-Wilson (PKW) algebra and critical factorization of the three-spin correlations in iron

Conventional neutron magnetic scattering is determined by two-spin correlation function and depends on one momentum \mathbf{Q} . However in the strong correlated spin systems there are n -spin nontrivial correlations where $n > 2$, which depend on $n - 1$ momenta q_i . The PKW algebra deals with n -spins correlations near the second order phase transition. It predicts that, if one momentum, say q_1 , is much larger than others $q_{i \neq 1}$ and the inverse correlation length $\kappa = \zeta^{-1}$, then the dependence on q_1 appears as a factor q^{-x} , where $x = 5 - \eta - 1/\nu$, where η and ν are the Fisher's and the correlation length exponents respectively [48–51]. This phenomenon may be called as a critical factorization. In the case of chiral scattering along with the momentum transfer \mathbf{Q} we have the momentum of the uniform magnetic field which is zero. The field \mathbf{H} is conjugated to the total magnetisation which is relevant variable for ferromagnets. As a result on the base of static and dynamic scaling theories for cubic ferromagnets we have [37]:

$$\text{Im } S(Q, \omega) = \frac{g\mu H}{T_c(Qa)^x(Qa)^y} \left[\frac{\omega}{T_c(Qa)^z} \right]. \quad (17)$$

Here H is the internal magnetic field, a is of order of interatomic distance, $y = (1/\nu) - (1 + \eta)/2$, $\kappa = a^{-1}\tau^\nu$, $\tau = (T - T_c)/T_c$ and z is the dynamical critical exponent. From this expression we see that if $Q \gg \kappa$, the chiral scattering is proportional to $\tau^{-1+\nu(1+\eta)/2} \simeq \tau^{-0.67}$, where in the right hand we put $\eta = 0$ and $\nu \simeq 2/3$.

This result was confirmed using original method for investigation the small-angle chiral scattering [52,53]. Corresponding results for $k_i\vartheta \gg \kappa$ are shown in Fig. 13 [48]. They are fitted by $\tau^{-\nu y}$ where $\nu y = 0.67 \pm 0.07$ in an agreement with the PKW algebra predictions. To our knowledge this is the only experimental confirmation of this algebra.

4.2. Crossover to dipolar spin dynamics in the chiral channel

It is well-known that the exchange approximation is not applicable for critical dynamics of ferromagnets near T_c in the region determined by the conditions [52,54]

$$4\pi\chi \gg 1; \quad Q < q_d = \left[4\pi(g\mu_B)^2 a^{-5} \right]^{1/2}, \quad (18)$$

where χ is the static magnetic susceptibility and q_d is the dipolar wave-vector. In this region the magnetic dipolar interaction plays crucial role due to demagnetization of the critical fluctuations. As a result there are two characteristic energies of the critical fluctuations: the exchange one $\Omega_e(Q) = T_c(Qa)^{z_e}$, where $z_e = (5 - \eta)/2 \simeq 2.5$ and the dipolar one $\Omega_d = T_c(q_d a)^{z_e - z_d}(Qa)^{z_d}$ with new dipolar critical exponent z_d .

Unsuccessful was an attempt to observe the crossover to dipolar dynamics using neutron scattering in iron [55]. In Fig. 14 results are shown for the chiral scattering in iron near T_c , where $P_s = \vartheta\sigma_{ch}(\vartheta)/\sigma(\vartheta)$ and $q_i = a^{-1}[2E/(T_c k_i a)]^{2/3}$ [42]. Qualitative explanation of these results is given in [37]. For $k_i\vartheta > q_i$ the scattering is inelastic and $P_s \sim (k_i\vartheta)^{-2}$. There is a crossover to quasielastic scattering at $k_i\vartheta \sim q_i$ and for $\kappa < k_i\vartheta < q_i$ one has

$$P_s \sim \vartheta\Omega(k_i\vartheta) / \Omega_e(k_i\vartheta), \quad (19)$$

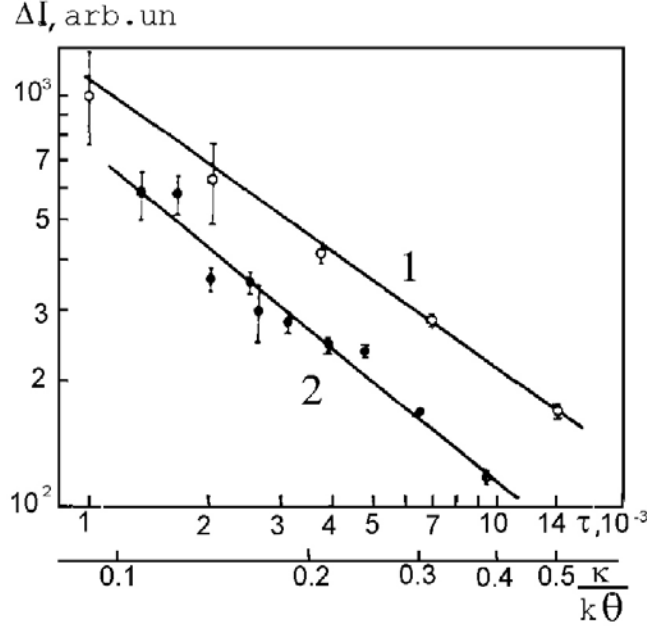


Figure 13: Temperature dependence of the integrated DC scattering in iron. (1) $\psi = 55^\circ$; (2) $\psi = 68^\circ$; τ and κ are defined in the text

where $\Omega(k; \vartheta)$ is a characteristic energy of the critical fluctuations. Hence, in the exchange approximation $P_s \sim \vartheta$ (dashed line in Fig.14). However there is the second maximum approximately at q_d . This maximum may be explained, if $z_d < 3/2$. According to Ref. [54] one has $z_d = z_e - 1/\nu \simeq 1$. Hence, we have qualitative experimental confirmation of this theoretical prediction. It should be pointed out that the value of z_d was calculated using the PKW algebra.

Very interesting results were obtained in the case of the spin-wave scattering in amorphous ferromagnets [46]. In this case methods of the conventional neutron spectroscopy are not very convenient, as there is no the Bragg scattering, and the inelastic small-angle scattering is masked by a huge elastic background connected to the spatial disorder. Neglecting the dipolar interaction for the spin-wave energy we have $\varepsilon_q = Dq^2$, where D is the spin-wave stiffness. Hence, the small-angle neutron scattering with excitation or absorption of the spin-waves may be considered as interaction of the heavy particle (neutron of the mass M) with the light one (spin-wave) and there is the cut-off angle $\vartheta_0 = 1/(2MD) \ll 1$. In Fig. 13 the small-angle scattering in amorphous alloy $\text{Fe}_{50}\text{Ni}_{22}\text{Cr}_{10}\text{P}_{18}$ below T_c is shown (Fig. 15a) along with its chiral part, which is very weak, by clearly seen as it changes sign with ϑ . The cut-off angle easily obtained from these data (Fig. 15b) and temperature dependence of the $\theta_0 (\sim 1/D)$ in critical region below T_c were determined (Fig. 15c). Very well agreement with the predictions of the dynamical scaling was demonstrated (critical exponent x in dependence $\theta_0 \sim \tau^{-x}$ is near $1/3$). Two dimensional picture of spin wave scattering is shown in Fig. 16. From the data like these, the parameters of spin waves are obtained with high accuracy [56].

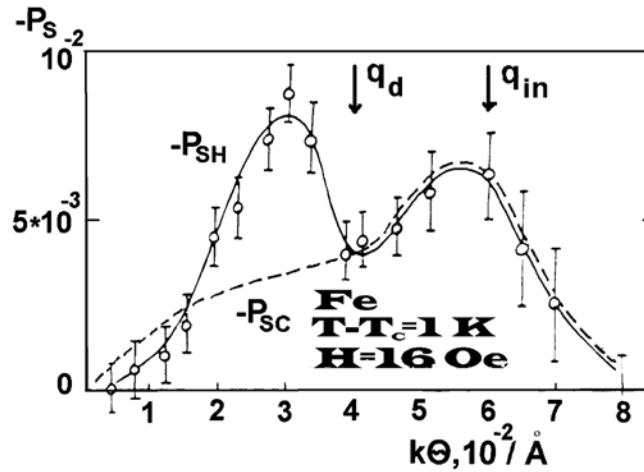


Figure 14: Crossover to dipolar critical dynamics in the chiral channels; κ , q_d and q_{in} are defined in the text. Dashed line shows the prediction in the exchange approximation

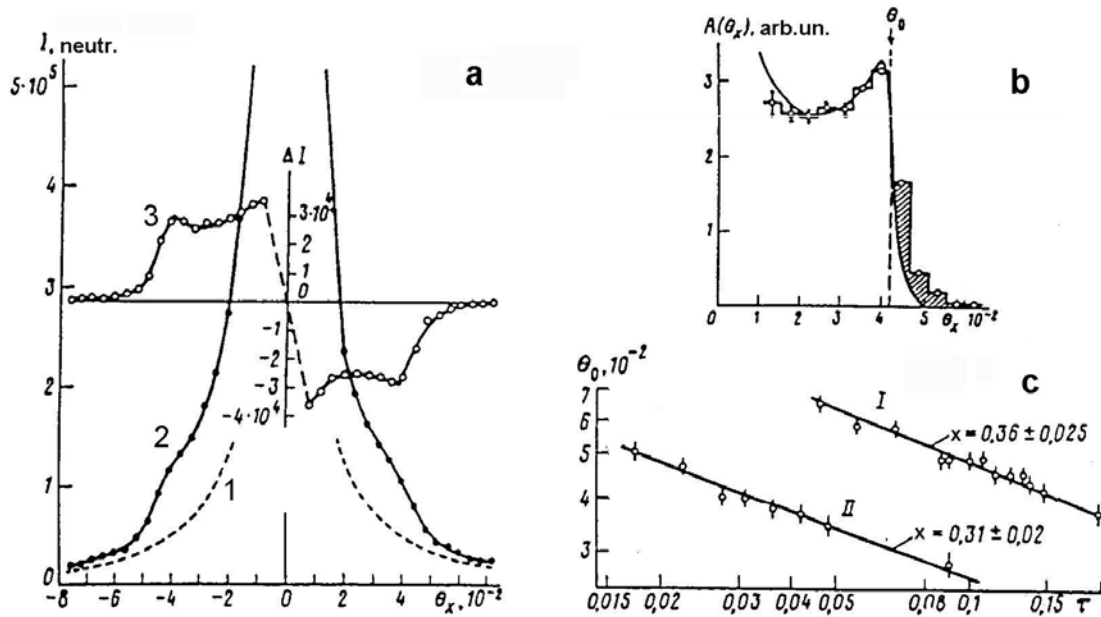


Figure 15: The scattering of polarized neutrons on spin waves in amorphous alloy $\text{Fe}_{50}\text{Ni}_{22}\text{Cr}_{10}\text{P}_{18}$: a) Intensity of direct beam (1), intensity of total scattering ($I_+ + I_-$) (2) and spin-dependence scattering $\Delta I = (I_+ - I_-)$ (3); b) Asymmetric part of scattering $A(\theta_x) = \frac{1}{2}[\Delta I(\theta_x) - \Delta I(-\theta_x)]$. Solid line is calculation with allowance for the angular resolution of the instrument, θ_0 is cut-off angle, the hatched region is effect of spin wave damping; c) The temperature dependence of cut-off angle $\theta_0 = E/Dk^2$ for samples $\text{Fe}_{50}\text{Ni}_{22}\text{Cr}_{10}\text{P}_{18}$ (I) and $\text{Fe}_{48}\text{Ni}_{34}\text{P}_{18}$ (II)

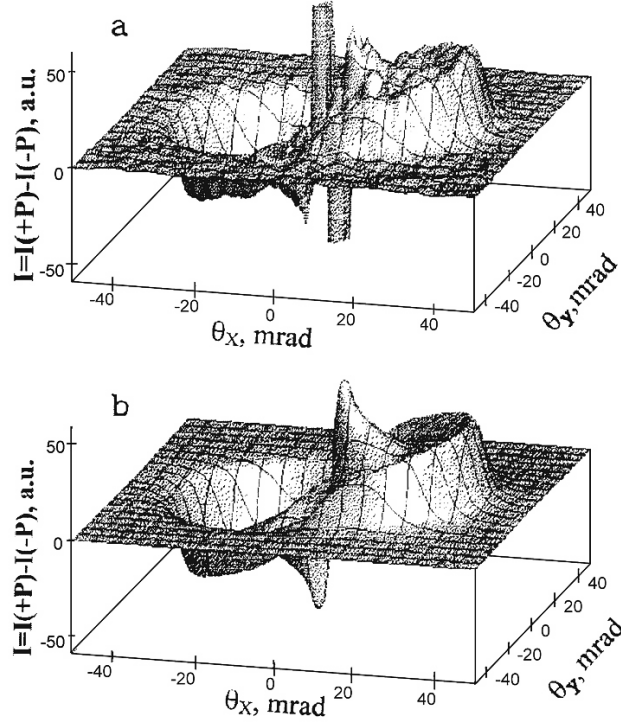


Figure 16: Spin wave antisymmetric scattering ΔI in the detector plane for $\text{Fe}_{50}\text{Ni}_{22}\text{Cr}_{10}\text{P}_{18}$; a) experimental picture and b) theoretical calculation with parameters from experimental data: spin wave stiffness $D = 52.74(5) \text{ meV \AA}^2$, damping $\Gamma_0(kR_c) = 25.2(5)$, dipole constant $\omega_0 \langle S \rangle = 50(3) \mu\text{eV}$

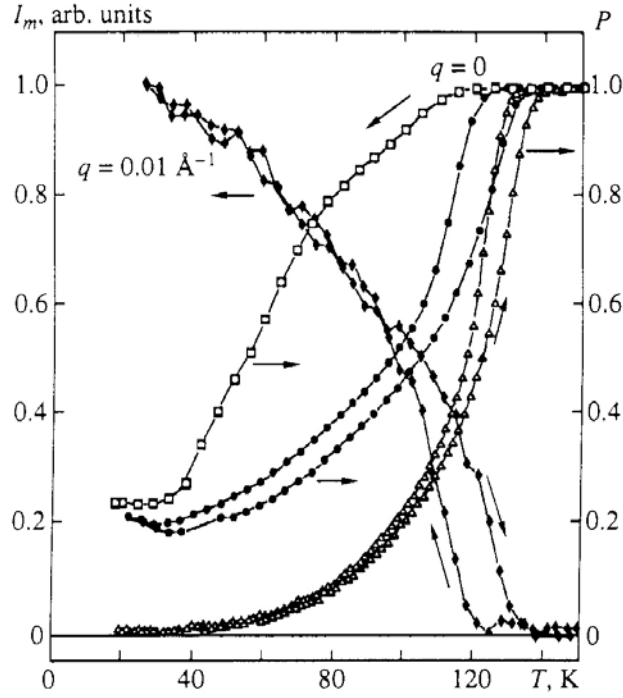


Figure 17: Temperature dependences of the polarization P in the central counter ($q < 0.003 \text{ \AA}^{-1}$) and the neutron magnetic scattering intensity I_m for and $\text{Sm}_{1-x}\text{Sr}_x\text{MnO}_3$ sample with $x = 0.4$ for $H = 0$ (\bullet , \diamond) and $H = 4.2 \text{ kOe}$ (Δ). The neutron depolarization data for the $x = 0.25$ sample (\square) for $H = 0$ are shown too

5. Problem of colossal magnetoresistance (CMR)

Interest in manganites ($\text{R}_{1-x}^{3+}\text{A}_{1-x}^2$) MnO_3 has increased in connection with the presence of colossal negative magnetoresistance as well as a lot of structural and magnetic phase transitions related to complicated intrinsic structure. Investigators have always called attention to the magnetic inhomogeneities of these systems and have conjectured that magnetic inhomogeneities are an inherent and fundamental feature of these materials and give rise to the CMR. In our small-angle polarized neutron scattering experiments on the powder sample $^{154}\text{Sm}_{1-x}\text{Sr}_x\text{MnO}_3$ ($x = 0.25; 0.4$) we have investigated the magnetic mesoscopic structure in the temperature range $T = 16 - 300 \text{ K}$ and applied magnetic field $H = 0 - 4200 \text{ Oe}$. In Ref. [57] it was found that the system possessed a distorted perovskite structure and: (i) at $x = 0.4$ a transition into magnetically ordered phase ($110 - 130 \text{ K}$) along with insulator-metal transition were observed; (ii) at $x = 0.25$ a rapid growth of the magnetic susceptibility ($90 - 100 \text{ K}$) was observed without changing of conductivity. In these experiments we obtain the temperature and applied field dependence of small-angle intensity $I(T)$, polarization $P(T)$ and intensity of magnetic-nuclear interference scattering.

The typical dependence $I_m(T)$ and $P(T)$ at different H are shown in Fig. 17. The total magnetic cross section $\Sigma(t)$ on large scale ferromagnetic correlations under various measuring conditions are shown in Fig. 18.

The cross section $\Sigma(T)$ was obtained from depolarization of the transmitted neutrons to the

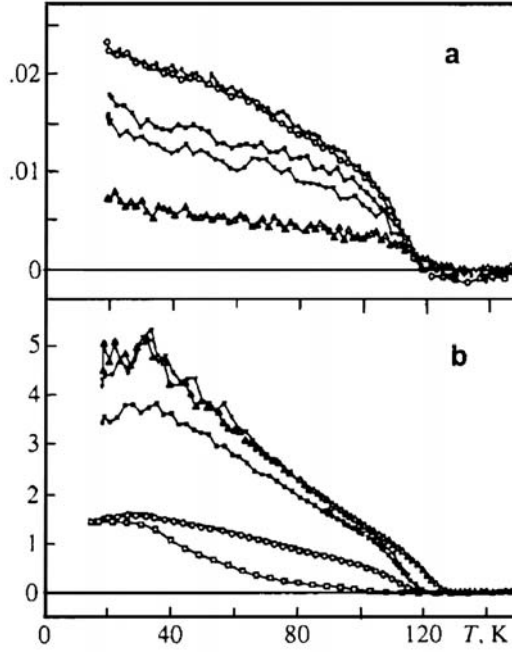


Figure 18: Temperature dependences of (a) the magnetic scattering intensity I_m with $q = 0.01 \text{ \AA}^{-1}$ and (b) the integrated magnetic scattering in the range $q < 0.003 \text{ \AA}^{-1}$ for $\text{Sm}_{1-x}\text{Sr}_x\text{MnO}_3$ sample with $x = 0.4$ and $H = 0$ (\bullet), 130 (\circ), 800 (\square), 1240 (∇), 4200 Oe (Δ). The data for the $x = 0.25$ sample (\square) for $H = 0$ are shown too

central detector $P = P_0 \exp(-c\Sigma L)$, where c is a coefficient, L is the thickness of the samples). One can see: (i) there is very broad transition region T with a characteristic range in $P(T)$ and $\Sigma(T)$; (ii) the temperature hysteresis in $P(T)$ and $I(T)$ is observed; (iii) $P(T)$ at $H = 0$ is not decreased to zero. Analysis of the dependences $I(q)$ showed that they are well described by the quadratic Lorentzian $I(q) = A(q^2 + k^2)^{-2}$, where A and $k = 1/R_c$ are parameters. It was shown in these experiments, that the low-temperature magnetic state of Sm system can be characterized as very strong magnetic disordering by fluctuations with size $R_c = 180 - 250 \text{ \AA}$. Moreover, these fluctuations merge with clusters with $(4 - 5)R_c$ or more in size. Only this scenario allows to explain $P(T)$ data, whereas the depolarization on the fluctuations with scale R_c is too small to describe the experimental data.

In conclusion we would like to thank the scientists and white-collar workers who take part in performing mentioned theoretical and experimental works. Part of them one can see in the list of the used publications.

References

- [1] A.I. Akhiezer, I.Ya. Pomeranchuk, *Certain problems of nuclear theory* (in Russian), Gostekhizdat, 1950.
- [2] S.V. Maleyev, J.Eksp.Teor.Fiz. **40**, 860 (1961); Sov.Phys.JETP **13**, 860 (1961).
- [3] Yu.A. Izyumov, S.V. Maleyev, J.Eksp.Teor.Fiz. **41**, 1644 (1961) ; Sov.Phys. JETP **14**, 1168 (1962).
- [4] S.V. Maleyev, V.G. Baryakhtar, R.A. Suris, Fiz.Tv.Tela **4**, 3461 (1962); Sov.Phys. Solid St. **4**, 2533 (1963).
- [5] M. Blume, Phys.Rev. **130**, 1670 (1963).
- [6] R.M. Moon, T. Riste, W.C. Koehler, Phys.Rev. **181**, 920 (1969) .
- [7] M.Th. Rekveldt, J.de Phys. **C132** , 579 (1971).
- [8] A.I. Okorokov, V.V. Runov, G.M. Drabkin, *Method of ascertainment of neutron beam polarization*. Copyright certificate No.408247 with priority from 10.03.72. Information bulletin **47** (1973) 9; *Device for analysis of magnetic structure of ferro- and ferrimagnetic materials*. Copyright certificate No.447093 with priority from 03.04.72. Information bulletin **5** (1976).
- [9] G.M. Drabkin, A.I. Okorokov, V.V. Runov, *Anisotropy of neutron beam depolarization* Pis'ma v Zh.Eksp.Teor.Fiz. **15**, 458 (1972) ; Sov.Phys. JETP Lett. **5**, 324 (1972).
- [10] F. Tasset, Physica **B 56–157**, 627 (1989).
- [11] G.M. Drabkin, E.I. Zabidarov, Ya.I. Kasman, A.I. Okorokov, *Critical scattering of polarized neutrons on Ni*, Pis'ma v Zh.Eksp.Teor.Fiz. **2**, 541 (1965); Sov.Phys. JETP Lett. **2**, 335 (1965) .
- [12] O. Halpern, M.H. Johnson, *On the magnetic scattering of neutrons*, Phys.Rev. **55**, 898 (1939).
- [13] S.V. Maleyev, *On polarized neutron scattering near phase transition temperature*, Pis'ma v ZhETF **2**, 545 (1965); Sov.Phys. JETP Lett. **2**, 338 (1965).
- [14] M.F. Collins, V.J. Minkiewicz et al., *Critical and spin-wave scattering of neutrons from iron*, Phys.Rev. **179**, 417 (1969).
- [15] B.P. Toperverg, V.V. Runov, A.I. Okorokov, A.G. Gukasov, *The investigation of double critical magnetic scattering in polarized neutron experiments*, Phys.Lett. **71A**, 289 (1979).
- [16] D. Bally, E. Grabcev, M. Popovici et al., J.Appl.Phys. **39**, 459 (1968).
- [17] P. Parette, R. Kahn, J.Phys. **32**, 447 (1971).
- [18] P. Resibois and C. Piette, Phys.Rev.Lett. **24**, 514 (1970) .
- [19] P. Resibois and C. Piette, Phys. Lett. **42A**, 531 (1973).
- [20] C.J. Glinka, J. Minkiewicz, L. Passel, *Small-angle critical neutron scattering from cobalt*, Phys.Rev. **B16**, 4084 (1977) .

- [21] J.P. Wicksted, P. Böni, G. Shirane, Phys.Rev. **B30**, 3655 (1984).
- [22] S.V. Maleyev, Sov.Phys. JETP **46**, 826 (1977).
- [23] O. Halpern, T. Holstein, Phys.Rev. **59**, 960 (1941).
- [24] S.V. Maleyev, V.A. Ruban, *On critical depolarization of neutrons traversing a ferromagnetic body*, J. Eksp. Teor. Fiz. **62**, 416 (1972); Sov. Phys. JETP **35**, 222 (1972).
- [25] S.V. Maleyev, V.A. Ruban, *An analysis of the domain structure of the ferromagnets by means of neutron depolarization*, Fiz. Tv. Tela **18**, 2283 (1976); Sov.Phys. Solid State **18**, 1331 (1976) .
- [26] S.V. Maleyev, J. Phys. (France) **43C** 7, 23 (1982).
- [27] G.P. Gordeev, I.M. Lazebnik, L.A. Akselrod, *Anisotropy of neutron depolarization in diluted alloy PdFe near transition*, Fiz. Tv. Tela **18**, 2059 (1976).
- [28] A.I. Okorokov, A.G. Gukasov, I.M. Otchik, V.V. Runov, *Experimental observation of the asymmetry of polarized neutron critical scattering from Fe above T_c* , Phys. Lett. **65A**. 60 (1978).
- [29] S.V. Grigoriev, S.A. Klimko, S.V. Maleyev, A.I. Okorokov, V.V. Runov, D.Yu. Chernyshov, *Investigation of magnetic phase transition in FCC iron-nickel alloys*, JETP **112**. 1 (1997).
- [30] S.V. Grigoriev, S.V. Maleyev, A.I. Okorokov, V.V. Runov, *Observation of two scale lengths of magnetic correlations in FeNi alloy above T_c* , Phys. Rev. **B58**, 3206 (1998).
- [31] S.V. Grigoriev, S.A. Klimko, W.H. Kraan, M.I. Rekveldt, A.I. Okorokov, V.V. Runov, *Magnetic phase transition in a disordered FeNi alloy: percolative scenario*, Physica **B276**, 556 (2000).
- [32] L.a. Akselrod, G.P. Gordeev, V.N. Zabenkin, M.R. Kolkhidashvili, I.M. Lazebnik, *Measurement of the distribution of trapped flux in a Josephson-coupled medium by neutron polarimetry*, Physica **C221**, 219 (1994).
- [33] A.M. Campbell and J.E. Evetts, *Critical currents in Superconductors* (Taylor and Francis, London, 1972).
- [34] J.R. Clem and A. Perez-Gonzales, Phys.Rev. **B33**, 1601 (1986).
- [35] G.P. Gordeev, L.A. Akselrod, S.L. Ginzburg, V.N. Zabenkin, I.M. Lazebnik, *The application of polarized neutrons for visualization of longitudinal and transverse currents in a Josephson medium*, Physica **B234–236**, 832 (1997).
- [36] V.V. Runov, S.L. Ginzburg, B.P. Toperverg, A.D. Tretyakov, A.I. Okorokov and E.I. Mal'tsev, *Investigation of spin correlations in concentrated Fe-Ni-Cr spin glasses by the method of polarized neutron scattering*, Zh. Eksp. Teor. Fiz. **94**, 325 (1988); Sov. Phys. JETP **67**, 181 (1988).
- [37] A.V. Lazuta, S.V. Maleyev, B.P. Toperverg, Zh. Eksp. Teor. Fiz. **81**, 1475 (1981); Sov. Phys. JETP **54**, 782 (1981).
- [38] S.V. Maleyev, Phys.Rev.Lett. **75**, 4682 (1995).

- [39] V.P. Plakhty, S.V. Maleyev, J. Kulda, J. Wosnitza, D. Visser, R.K. Kremer, E. Moskvina, Europhys.Lett. **40**, 215 (1999).
- [40] V.P. Plakhty, J. Kulda, V. Visser, E. Moskvina, J. Wosnitza, Phys.Rev.Lett. **85**, 3942 (2000).
- [41] V.P. Plakhty *et al.*, in this Edition, p.160.
- [42] A.I. Okorokov, A.G. Gukasov, V.V. Runov *et al.*, *Asymmetry of polarized neutron critical scattering and the critical dynamics of ferromagnets above T_c in magnetic field*, Zh. Eksp. Teor. Fiz. **81**, 1462 (1981); Sov. Phys. JETP **51**, 775 (1981).
- [43] A.G. Gukasov, A.I. Okorokov, F. Fujara, O. Schärpf, *About possibility to study β -spin correlation dynamics in ferromagnets above T_c by method of pseudorandom modulation of neutron polarization*, Pis'ma Zh. Eksp. Teor. Fiz. **37**, 432 (1983).
- [44] S. Maleyev, V. Plakhty, O. Smirnov *et al.* *The first observation of dynamical chirality by means of polarized neutron scattering in the triangular lattice antiferromagnet CsMnBr₃*, J.Phys.: Condens. Matter **10**, 951 (1998).
- [45] A.I. Okorokov, A.G. Gukasov, V.V. Runov, M. Roth, *Polarization effects in the scattering of cold neutrons from iron above T_c* , Sol. St. Comm. **38**, 583 (1981).
- [46] A.I. Okorokov, V.V. Runov, B.P. Toperverg *et al.*, *Study of spin waves in amorphous magnetic materials by polarized neutron scattering*, Pis'ma Zh. Eksp. Teor. Fiz. **43**, 390 (1986); Sov.Phys. JETP Lett. **43**, 503 (1986).
- [47] A.I. Okorokov, A.G. Gukasov, V.V. Runov, M. Roth, S.V. Maleyev, *The asymmetry of polarized neutron critical scattering from Fe above T_c in magnetic field*, J. Physique Suppl. **43C** 7, 91 (1982).
- [48] A.M. Polyakov, Sov. Phys. JETP **30**, 151 (1970).
- [49] L.P. Kadanoff, Phys. Rev. Lett. **23**, 1430 (1969).
- [50] K.G. Wilson, Phys.Rev. **D3**, 1818 (1971).
- [51] S.V. Maleyev, *Critical dynamics of ferromagnetic materials*, in: I.M. Khalatnikov (Ed.), Sov. Physics Reviews **8**, 323 (1987).
- [52] A.I. Okorokov, A.G. Gukasov, V.N. Slusar, B.P. Toperverg, O. Schärpf, F. Fujara, *Investigation of critical factorisation of triple dynamic spin correlations by means of polarized neutron scattering in Fe above T_c* , Pis'ma Zh. Eksp. Teor. Fiz. **37**, 269 (1983); Sov. Phys. JETP Lett. **37**, 319 (1983).
- [53] A.V. Lazuta, C.V. Maleyev, B.P. Toperverg, *About triple dynamic correlation of magnetization fluctuations in ferromagnetics and the possibility of its study of means of polarized neutrons*, Zh. Eksp. Teor. Fiz. **75**, 764 (1978).
- [54] S.V. Maleyev, Sov. Phys. JETP **39**, 889 (1974).
- [55] F. Mezei, Phys. Rev. Lett. **49**, (10961982).

- [56] B.P. Toperverg, V.V. Deriglazov, V.E. Mikhailova, *On the studies of spin-wave dynamics in ferromagnets by polarized neutron scattering*, Physica **B183**, 326 (1993).
- [57] V.V. Runov, D.Yu. Chernyshov, A.I. Kurbakov, M.K. Runova, V.A. Trunov, and A.I. Okorokov, *Mesoscopic magnetic inhomogeneities in the low-temperature phase and structure of $\text{Sm}_{1-x}\text{Sr}_x\text{MnO}_3$ ($x < 0.5$) perovskite*, Zh. Eksp. Teor. Fiz. **118**, 1174 (2000) 7; Sov.Phys. JETP **91**, 1017 (2000).